*The British Journal of Radiology, 85* (2012), 29–36

# The effect of gadoxetic acid enhancement on lesion detection and characterisation using $T_2$ weighted imaging and diffusion weighted imaging of the liver

[1,2]S A CHOI, MD, [1]S S LEE, MD, PhD, [3]I-H JUNG, BA, [3]H A KIM, BA, [1]J H BYUN, MD, PhD and [1]M-G LEE, MD, PhD

[1]*Department of Radiology and Research Institute of Radiology, University of Ulsan College of Medicine, Asan Medical Center, Seoul, Republic of Korea,* [2]*Eulji College of Medicine, University of Eulji, Seoul, Republic of Korea, and* [3]*University of Ulsan College of Medicine, Seoul, Republic of Korea*

**Objectives**: To evaluate the effect of gadoxetic acid enhancement on the detection and characterisation of focal hepatic lesions on $T_2$ weighted and diffusion weighted (DW) images.
**Methods**: A total of 63 consecutive patients underwent $T_2$ weighted and DW imaging before and after gadoxetic acid enhancement. Two blinded readers independently identified all of the focal lesions using a five-point confidence scale and characterised each lesion using a three-point scale: 1, non-solid; 2, indeterminate; and 3, solid. For both $T_2$ weighted and DW imaging, the accuracies for detecting focal lesions were compared using the free-response receiver operating characteristic analysis; the accuracies for lesion characterisation were compared using the McNemar test between non-enhanced and gadoxetic acid-enhanced image sets. For hepatic lesions $\geqslant$1 cm, the lesion-to-liver contrast-to-noise ratio (CNR) and the apparent diffusion coefficient (ADC) were compared in the non-enhanced and enhanced image sets using the generalised estimating equations.
**Results**: For both $T_2$ weighted and DW images, the accuracies for detecting focal lesions ($p \geqslant 0.52$) and those for lesion characterisation ($p \geqslant 0.63$) did not differ significantly between the non-enhanced and enhanced image sets. The lesion-to-liver CNR was significantly higher on enhanced DW images than on non-enhanced DW images ($p = 0.02$), although the difference was not significant for $T_2$ weighted imaging ($p = 0.65$). The mean ADC values of lesions did not differ significantly on enhanced and non-enhanced DW imaging ($p = 0.75$).
**Conclusion**: The acquisition of $T_2$ weighted and DW images after administration of gadoxetic acid has no significant effect on the detection or characterisation of focal hepatic lesions, although it improves the lesion-to-liver CNR on DW images.

Received 11 March 2010
Revised 25 April 2010
Accepted 28 April 2010

DOI: 10.1259/bjr/12929687



Various contrast agents have been developed and utilised for MRI of the liver in order to facilitate the detection and characterisation of focal hepatic lesions. Gadoxetic acid (gadolinium-ethoxybenzyl-diethylene-triamine pentaacetic acid, Primovist®; Bayer Schering Pharma, Berlin, Germany) is a recently developed, liver-specific contrast agent. As it has combined extracellular and hepatocyte-specific properties, gadoxetic acid can provide functional information regarding the cellular composition of focal hepatic lesions on hepatobiliary phase imaging as well as haemodynamic information on dynamic MRI following bolus injection. These properties of gadoxetic acid have been reported to improve the accuracy of liver MRI for lesion detection and characterisation [1–7].

Address correspondence to: Professor Seung Soo Lee, Department of Radiology and Research Institute of Radiology, University of Ulsan College of Medicine, Asan Medical Center, 388-1 Poongnap2-Dong, Songpa-Gu, 138-736 Seoul, Republic of Korea. E-mail: seungsoolee@amc.seoul.kr

By contrast, these advantages of gadoxetic acid-enhanced liver MRI are obtained with increased examination time, as delayed scanning approximately 20 min after contrast administration is necessary for optimal hepatobiliary phase imaging [4, 5, 7–9]. Among the pulse sequences commonly acquired for clinical liver MRI, $T_2$ weighted and diffusion weighted (DW) imaging are frequently performed using a respiratory-triggered method in order to improve image quality [10–12], thus a lengthy acquisition time is required. To shorten the examination time for gadoxetic acid-enhanced MRI, it has been proposed to perform respiratory-triggered $T_2$ weighted and DW imaging during the interval between dynamic $T_1$ weighted imaging and the hepatobiliary phase imaging [7, 13, 14]. However, this modification in the MRI protocol is only feasible if the administration of gadoxetic acid does not degrade the image quality and provides comparable image quality and accuracy to non-enhanced imaging.

Although previous studies have demonstrated that gadolinium-enhanced $T_2$ weighted images improve the

conspicuity of focal hepatic lesions compared with unenhanced $T_2$ weighted images [15, 16], these studies used non-specific extracellular contrast agents. Considering the different properties of extracellular contrast agents and gadoxetic acid, these results might not be easily applied to gadoxetic acid-enhanced MRI.

Therefore, the purpose of our study was to evaluate the effect of gadoxetic acid on lesion detection and characterisation using $T_2$ weighted and DW imaging.

## Methods and materials

### *Patients*

The study protocol was approved by our institutional review board and informed consent was obtained from each participant. From January to May 2008, a total of 85 consecutive patients underwent gadoxetic acid-enhanced liver MRI to evaluate focal hepatic lesions. Among these patients, 22 were excluded for several reasons: the presence of more than 10 hepatic lesions (because of the difficulty in comparing numerous lesions depicted on non-enhanced images and those on gadoxetic acid-enhanced images) ($n$=10); an inability to obtain proof of the hepatic lesion ($n$=8); unacceptable image quality owing to motion artefacts ($n$=2); or failure to perform the MRI according to our research protocol ($n$=2). The remaining 63 patients formed the study population, which included 46 males (mean age 56.3 years; range 31–83 years) and 17 females (mean age 55.0 years; range 37–79 years).

### *MR examination*

MRI was performed using a 1.5 T scanner (Magnetom Avanto; Siemens, Erlangen, Germany) with a six-element, phased-array body coil as the receiver. The MRI protocol used in our study is summarised in Figure 1. All patients underwent $T_2$ weighted imaging and DW imaging before and after administration of gadoxetic acid; gadoxetic acid-enhanced $T_2$ weighted and DW imaging were performed immediately after completion of dynamic $T_1$ weighted imaging and after 10 min delayed hepatobiliary phase imaging, respectively.

$T_2$ weighted imaging was performed using a respiratory-triggered, turbo spin-echo sequence with the following scan parameters: repetition time (TR)/echo time (TE) 2664–5755 ms (depending on the patient's respiratory cycle)/82 ms; section thickness 6 mm; intersection gap 1.2 mm; matrix 384 × 190; echo train length 9; number of signal averages 2; and mean acquisition time 4.6 min. DW images were acquired using a respiratory-triggered, single-shot echo planar sequence with diffusion weighted gradients (*i.e.* *b*-factors of 0, 50, 300, 600 and 900 s mm$^{-2}$) applied in three orthogonal directions. The scan parameters for DW imaging were as follows: TR/TE 4000 ms/80 ms; section thickness 6 mm; intersection gap 1.2 mm; matrix 192 × 162; echo train length 123; number of signal averages 4; parallel imaging technique (GRAPPA; Siemens Medical Solutions) used with an acceleration factor of 2; and mean acquisition time 5.3 min. For both $T_2$ weighted and DW imaging, fat saturation was achieved using the chemical shift-selective fat suppression technique. The rectangular field of view was used.

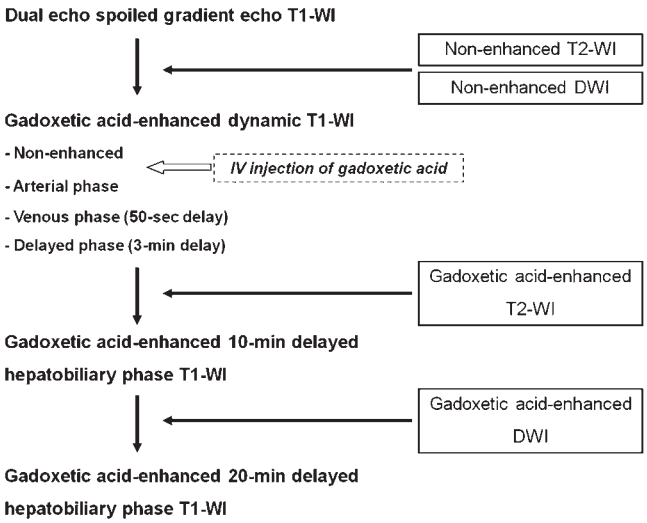


**Figure 1.** Flow diagram summarising the MRI protocol.

After the non-enhanced $T_1$ weighted images were acquired using a fat-suppressed, three-dimensional, spoiled-gradient echo sequence (VIBE; Siemens), 10 ml of gadoxetic acid was administered as an intravenous bolus followed by a 30 ml saline flush (at a rate of 2 ml s$^{-1}$ using a power injector in the arterial phase). The images were obtained in the arterial phase which was determined using a real-time bolus display method in the venous phase (50 s after contrast injection), delayed phase (3 min following contrast injection) and in the hepatobiliary phases (10 min and 20 min after contrast injection).

### *Qualitative image analysis*

Qualitative image analysis was performed independently by two, board-certified radiologists (with 7 years and 1 year, respectively, of clinical experience interpreting liver MRI) in a blinded manner during two separate sessions; the readers interpreted the $T_2$ weighted images during the first session and the DW images during the second session. For each review session, 126 image sets (*i.e.* 63 non-enhanced and 63 gadoxetic acid-enhanced image sets) were presented in random order. Patient data and the imaging parameters were removed from the images. The readers were blinded to the number and final diagnoses of both the hepatic lesions and MRI acquisition conditions (*i.e.* non-enhanced or gadoxetic acid-enhanced).

For each review session, the readers identified all of the focal hepatic lesions. They recorded the segmental location and size of each lesion and graded the readers' confidence level for the presence of each lesion using a five-point confidence scale: 1, confidence <25%; 2, 25%≤ confidence <50%; 3, 50%≤ confidence <75%; 4, 75%≤ confidence <90%; and 5, confidence ⩾90%. The readers then characterised each detected focal lesion using a three-point scale: 1, non-solid; 2, indeterminate; and 3, solid. Non-solid lesions represented haemangioma and hepatic

cysts, while the other focal hepatic lesions were regarded as solid lesions. On $T_2$ weighted images, a lesion showing high signal intensity (SI) similar to that of cerebrospinal fluid was considered non-solid, whereas a lesion with an SI lower than that of cerebrospinal fluid was considered solid [17]. On DW images, a lesion was regarded as non-solid if it showed homogeneously high SI on DW images at $b=0$ and 50 s mm$^{-2}$ with an apparent SI decrease on DW images at $b=600$ and 900 s mm$^{-2}$ [12]. A lesion was considered solid if it was mildly to moderately hyperintense on DW images at $b=0$ and 50 s mm$^{-2}$ and remained hyperintense at $b=600$ and 900 s mm$^{-2}$ [12].

After completing the qualitative image analysis, the two readers reviewed in consensus all available MRIs, follow-up imaging examinations, the patients' clinical data and the pathology reports and constructed the reference standard for focal hepatic lesions by combining all of this information.

### Quantitative image analysis

Quantitative analysis was performed by one radiologist (blinded) on a commercially available workstation (Syngo; Siemens Medical Solutions). The reader performed operator-defined region of interest (ROI) measurement of the SI of the liver ($SI_{liver}$) and the focal hepatic lesion ($SI_{lesion}$), as well as recording the standard deviation (SD) of background noise ($SD_{noise}$) for each of the non-enhanced and gadoxetic acid-enhanced $T_2$ weighted and DW images. Quantitative analysis of the DW images was performed at $b=50$ s mm$^{-2}$, as DW images obtained at a low $b$-factor (*i.e.* a $b$-factor of 50–150) are commonly used to detect focal hepatic lesions [12]. Quantitative analysis of focal hepatic lesions [*i.e.* measurement of the SI and the apparent diffusion coefficient (ADC) value of the lesions] was only performed for target lesions, which included focal hepatic lesions 10 mm or larger in diameter, in order to minimise any inaccuracies in quantitative analysis resulting from the partial volume averaging effect.

The SI of the liver was measured by averaging the SI values of 4, 1.5 cm, circular ROIs; each ROI was placed at each of the right and left hepatic lobes on each of the 2 image slices and were positioned in areas devoid of large vessels and prominent artefacts. The SD of the background noise was measured by averaging the SD values of the two, largest possible, rectangular ROIs positioned in the phase-encoding direction outside the abdominal wall on the two image slices. The SI of the target lesion was measured by averaging the SI values of two circular ROIs, which were drawn to encompass as much of the lesion as possible on two consecutive image slices. Using the copy-and-paste function of the workstation, we could achieve a nearly complete match of the sizes and the locations of the ROIs in the non-enhanced and gadoxetic acid-enhanced images. The liver signal-to-noise ratio (SNR) was calculated as $SI_{liver}/SD_{noise}$. The lesion-to-liver contrast-to-noise ratio (CNR) was calculated as $(SI_{lesion}-SI_{liver})/SD_{noise}$.

The same radiologist performed the ROI measurement of the ADC values of the target lesions on DW images using MATLAB-based software (blinded), which automatically calculates ADC values of the areas within manually drawn ROIs [18]. For each target lesion, the ROI was placed in the same manner as the ROI measurement of the SI of the target lesion. The ADC was calculated by combining data for all of the $b$-values ($b=0$, 50, 300, 600 and 900 s mm$^{-2}$) using the linear regression analysis of the function of $S=S_0\exp(-b\times \mathrm{ADC})$, where $b$ is the diffusion factor, $S$ is the SI after applying the diffusion gradient and $S_0$ is the SI at $b=0$ s mm$^{-2}$.

### Statistical analysis

The diagnostic accuracy for detecting focal hepatic lesions was compared in the non-enhanced and the gadoxetic acid-enhanced image sets for both $T_2$ weighted and DW imaging, using a free-response receiver operating characteristic analysis. The analysis was performed using JAFROC1 analysis software version 1.0 (http://devchakraborty.com/) [19]; figure-of-merit values representing the diagnostic accuracy were compared in the non-enhanced and the gadoxetic acid-enhanced image sets for both $T_2$ weighted and DW imaging using the $F$-test. To evaluate the effect of gadoxetic acid enhancement on lesion characterisation, we identified focal hepatic lesions that were detected on both non-enhanced and gadoxetic acid-enhanced images by each of the two readers. We then evaluated the agreement in lesion characterisation between the non-enhanced and the gadoxetic acid-enhanced image sets for $T_2$ weighted and DW imaging, using the weighted $\kappa$ statistic: a weighted $\kappa$ value of $<0.2$ represents poor agreement; a value of 0.21–0.4 fair agreement; a value of 0.41–0.60 moderate agreement; a value of 0.61–0.80 good agreement; and a value of 0.81–1.0 excellent agreement [20]. The accuracies in the characterisation of detected focal hepatic lesions were calculated and compared in the non-enhanced and the gadoxetic acid-enhanced image sets for both $T_2$ weighted and DW imaging using the McNemar test.

For both $T_2$ weighted and DW imaging, liver SI, background noise and liver SNR were compared between the non-enhanced and gadoxetic acid-enhanced image sets using the paired $t$-test. We compared the lesion-to-liver CNR and the ADC values of the focal hepatic lesions between the non-enhanced and gadoxetic acid-enhanced image sets using the generalised estimating equations to account for data clustering (*i.e.* multiple lesions in a single patient). Statistical analysis was performed with SPSS 15.0 for Windows (SPSS, Chicago, IL); $p$-values $<0.05$ were considered statistically significant.

## Results

### Characteristics of focal hepatic lesions

A total of 173 focal hepatic lesions including 121 solid lesions (mean diameter 1.6 cm; range 0.5–6.7 cm) and 52 non-solid lesions (mean diameter 1.4 cm; range 0.5–7.1 cm) were identified in 63 patients. The final diagnoses and the methods used to diagnose focal hepatic lesions are summarised in Table 1. Of the 64 hepatocellular carcinomas, 45 were non-pathologically

**Table 1.** Summary of the final diagnosis of focal hepatic lesions and methods used to confirm the diagnosis

| Diagnosis | Total number of lesions | Pathological diagnosis | | Non-pathological diagnosis |
|---|---|---|---|---|
| | | Surgical resection | Ultrasound-guided biopsy | |
| Solid lesion | 121 | 21 | 10 | 90 |
| Hepatocellular carcinoma | 64 | 12 | 7 | 45 |
| Metastasis | 35 | 7 | 1 | 27 |
| Cirrhotic nodule | 10 | 0 | 1 | 9 |
| Ablated lesion | 5 | 0 | 0 | 5 |
| Cholangiocarcinoma | 3 | 2 | 1 | 0 |
| Eosinophilic infiltration | 4 | 0 | 0 | 4 |
| Non-solid lesion | 52 | 1 | 0 | 51 |
| Cyst | 27 | 0 | 0 | 27 |
| Haemangioma | 25 | 1 | 0 | 24 |

Data are number of lesions.

diagnosed according to the typical enhancement pattern seen on gadoxetic acid-enhanced MRI, the elevated serum α-fetoprotein and the increase in lesion size seen on follow-up CT or by the lipiodol uptake in the mass as seen on CT obtained after transarterial chemoembolisation. A total of 27 metastases were diagnosed by means of the typical findings on gadoxetic acid-enhanced MRI, as well as by the interval growth of the hepatic lesions on follow-up CT. Nine cirrhotic nodules were diagnosed according to their SI (variable SI on the $T_1$ weighted image and iso- or hypointensity on the $T_2$ weighted image) and enhancement pattern on gadoxetic acid-enhanced MRI (lack of hypervascular enhancement on the arterial phase image), while the stability of the lesion size was ascertained on follow-up MRI [21]. Four eosinophilic infiltrations in two patients were diagnosed according to the imaging findings (poorly defined lesions with faint hyperintensity on the $T_2$ weighted images and hypointensity on the venous phase images), the presence of peripheral eosinophilia and resolution of the hepatic lesions as seen on follow-up imaging examinations [22]. Three patients had five ablated lesions caused by previous radiofrequency ablation for hepatocellular carcinomas. Among the 52 non-solid lesions, 1 haemangioma was confirmed by surgical resection. The diagnosis of the remaining 24 haemangiomas and 27 cysts was made according to the pathognomonic findings on MRI and ultrasound.

### *Qualitative image analysis*

The results of the free-response characteristic analysis are summarised in Table 2. For both $T_2$ weighted and DW imaging, figure-of-merit values representing the diagnostic accuracies for detecting focal hepatic lesions did not differ significantly on the non-enhanced and gadoxetic acid-enhanced image sets for either reader ($p \geq 0.52$).

The agreement between each reader's lesion characterisation on non-enhanced image sets and that on gadoxetic acid-enhanced image sets was good to excellent for both $T_2$ weighted imaging ($\kappa = 0.92$ for reader 1 and 0.87 for reader 2) and DW imaging ($\kappa = 0.76$ for reader 1 and 0.84 for reader 2). The accuracies in lesion characterisation on $T_2$ weighted and DW images for all focal hepatic lesions ranged from 89.4% to 93.6% (Table 3). There was no statistically significant difference in the accuracies of lesion characterisation between non-enhanced and gadoxetic acid-enhanced image sets for both $T_2$ weighted and DW images for any lesion category ($p \geq 0.50$).

### *Quantitative image analysis*

Target lesions (*i.e.* focal hepatic lesions ⩾10 mm in diameter) included a total of 87 lesions (60 solid lesions and 27 non-solid lesions). Results of the quantitative analysis are summarised in Table 4. Liver SI and liver SNR were significantly higher on non-enhanced images than on gadoxetic acid-enhanced images for both $T_2$ weighted and DW imaging ($p \leq 0.001$) (Figures 2,3). Background noise was significantly higher on gadoxetic acid-enhanced $T_2$ weighted images than on non-enhanced $T_2$ weighted images ($p = 0.04$), whereas it did not differ significantly between non-enhanced and gadoxetic acid-enhanced DW images ($p = 0.82$). The lesion-to-liver CNR was significantly higher on gadoxetic acid-enhanced DW images than on non-enhanced DW images for all hepatic lesions and for solid hepatic lesions ($p \leq 0.04$), whereas it did not differ significantly on non-enhanced and gadoxetic acid-enhanced $T_2$ weighted images for any lesion category ($p \geq 0.32$) (Figures 2,3).

**Table 2.** Figure-of-merit values representing the diagnostic accuracies in detecting focal hepatic lesions

| | $T_2$ weighted imaging | | | Diffusion weighted imaging | | |
|---|---|---|---|---|---|---|
| | Non-enhanced | Gadoxetic acid-enhanced | *p*-values | Non-enhanced | Gadoxetic acid-enhanced | *p*-values |
| Reader 1 | 0.812 (0.770, 0.849) | 0.810 (0.760, 0.852) | 0.92 | 0.822 (0.772, 0.865) | 0.823 (0.774, 0.865) | 0.95 |
| Reader 2 | 0.862 (0.819, 0.897) | 0.877 (0.833, 0.912) | 0.52 | 0.823 (0.779, 0.861) | 0.818 (0.770, 0.860) | 0.81 |
| Average | 0.837 (0.798, 0.870) | 0.843 (0.803, 0.878) | 0.67 | 0.823 (0.782, 0.859) | 0.821 (0.779, 0.857) | 0.61 |

Data were obtained from the free-response receiver operating characteristic analysis. Data in parentheses represent 95% confidence intervals of figure-of-merit values.

**Table 3.** Accuracies in characterising focal hepatic lesions on non-enhanced and gadoxetic acid-enhanced $T_2$ weighted images and diffusion weighted images

| | | $T_2$ weighted imaging | | | Diffusion weighted imaging | | |
|---|---|---|---|---|---|---|---|
| | | Non-enhanced | Gadoxetic acid-enhanced | *p*-values | Non-enhanced | Gadoxetic acid-enhanced | *p*-values |
| Reader 1 | All | 93.3 (98/105) | 91.4 (96/105) | 0.63 | 91.2 (103/113) | 89.4 (101/113) | 0.79 |
| | Solid | 95.2 (60/63) | 92.1 (58/63) | 0.50 | 91.5 (65/71) | 88.7 (63/71) | 0.73 |
| | Non-solid | 90.5 (38/42) | 90.5 (38/42) | 1.00 | 90.5 (38/42) | 90.5 (38/42) | 1.00 |
| Reader 2 | All | 91.8 (101/110) | 93.6 (103/110) | 0.73 | 89.6 (103/115) | 89.6 (103/115) | 1.00 |
| | Solid | 92.4 (61/66) | 92.4 (61/66) | 1.00 | 88.6 (62/70) | 90.0 (63/70) | 1.00 |
| | Non-solid | 90.9 (40/44) | 93.2 (41/44) | 1.00 | 91.1 (41/45) | 88.9 (40/45) | 1.00 |

Accuracy values are percentages. Numbers in parentheses are the number of lesions.

The mean ADC values of the focal hepatic lesions measured on DW imaging obtained before and after gadoxetic acid enhancement [for all hepatic lesions ($n$=87) $1.6\times10^{-3}$ mm$^2$ s$^{-1}$ $\pm$0.6 *vs* $1.6\times10^{-3}$ mm$^2$ s$^{-1}$ $\pm$0.6 ($p$=0.75); for solid lesions ($n$=60) $1.3\times10^{-3}$ mm$^2$ s$^{-1}$ $\pm$0.3 *vs* $1.3\times10^{-3}$ mm$^2$ s$^{-1}$ $\pm$0.3 ($p$=0.89); for non-solid lesions ($n$=27) $2.3\times10^{-3}$ mm$^2$ s$^{-1}$ $\pm$0.6 *vs* $2.3\times10^{-3}$ mm$^2$ s$^{-1}$ $\pm$0.7 ($p$=0.75)] were nearly identical, resulting in no significant difference regardless of lesion category.

## Discussion

Our study demonstrated that the diagnostic accuracies of $T_2$ weighted and DW images acquired after administration of gadoxetic acid for detecting and characterising focal hepatic lesions were similar to those of standard non-enhanced images. The results of each reader's characterisation of hepatic lesions on non-enhanced images and those on enhanced images were in strong agreement, thus resulting in good to excellent agreement. Therefore, we assume that the administration of gadoxetic acid does not significantly affect the readers' visual interpretation of $T_2$ weighted and DW images.

Results of the quantitative image analysis show that administration of gadoxetic acid significantly decreases liver SI and consequently liver SNR for both $T_2$ weighted and DW images. Given the hepatocyte-specific property of gadoxetic acid, our findings might be attributable to the $T_2$ and $T_2$* shortening effect of the gadoxetic acid, which was taken up by the hepatocytes and

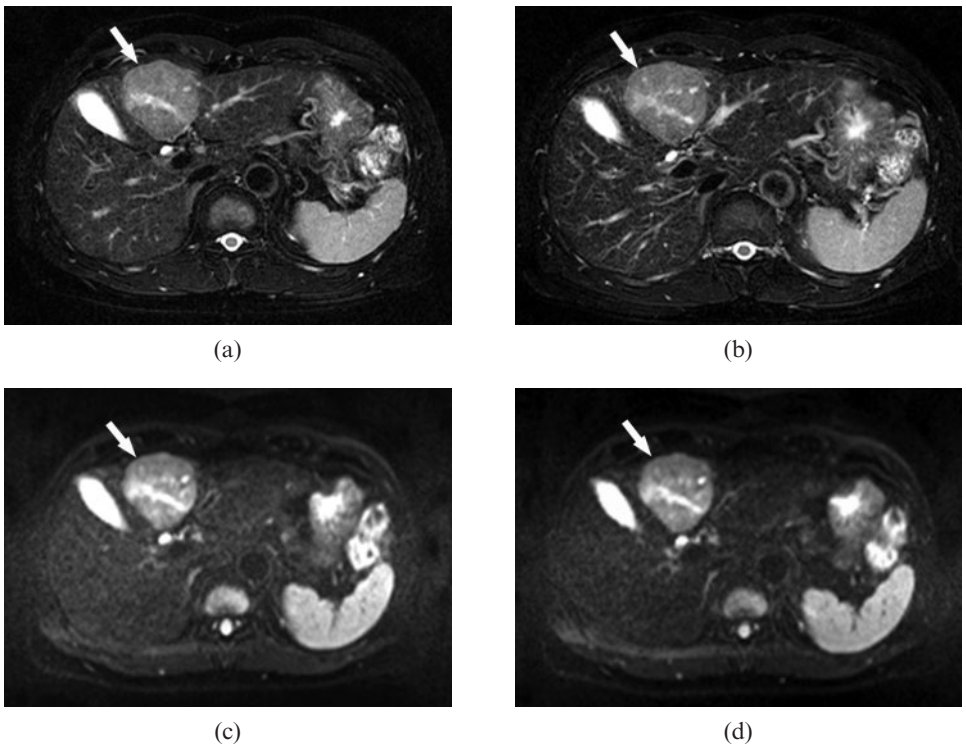


**Figure 2.** A 55-year-old male with hepatocellular carcinoma. (a, b) Fat-saturated, respiratory-triggered, $T_2$ weighted, turbo spin-echo axial images [repetition time (TR)/echo time (TE) 3850 ms/82 ms] acquired (a) before and (b) after administration of gadoxetic acid. The images demonstrate the hepatic mass in segment IV (arrows). The lesion-to-liver contrast is nearly identical for both images. (c, d) Fat-saturated, single-shot, echo-planar, diffusion weighted, axial images (TR/TE, 4000 ms/80 ms; *b*-factor, 50 s/mm$^2$) obtained (c) before and (d) after administration of gadoxetic acid show the same hepatic lesion (arrows). However, the liver signal intensity is slightly lower on (d) the image obtained after enhancement with gadoxetic acid than on (c) the non-enhanced image, resulting in slightly better lesion-to-liver contrast on (d) than on (c).

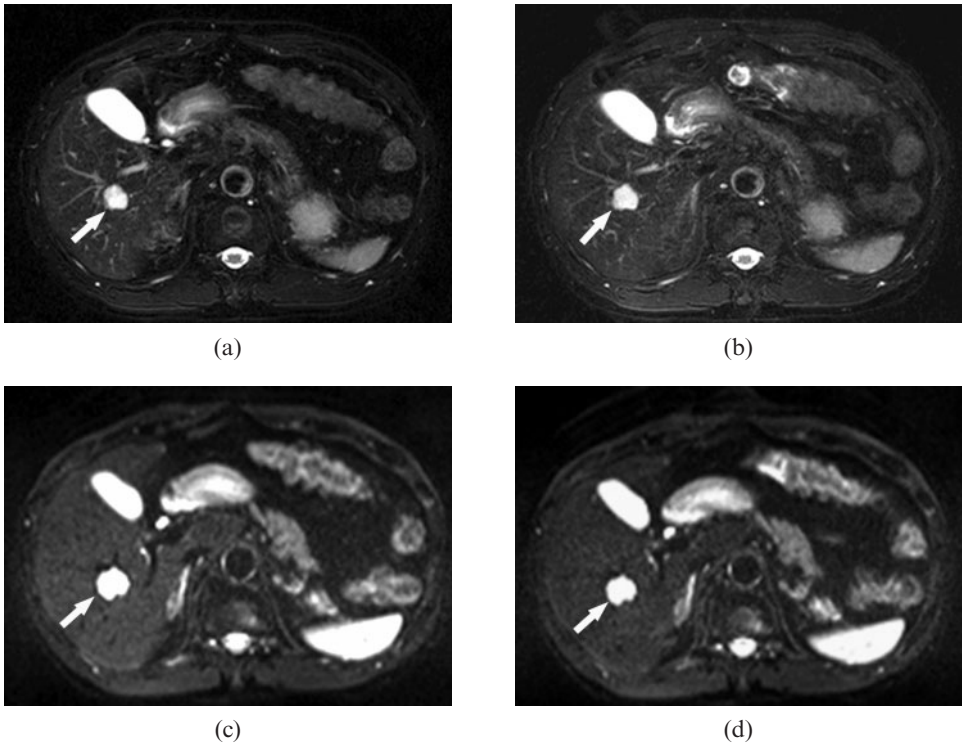

**Figure 3.** A 65-year-old male with haemangiomas. (a, b) Fat-saturated, respiratory-triggered, $T_2$ weighted, turbo spin-echo axial images [repetition time (TR)/echo time (TE) 3700 ms/82 ms] acquired (a) before and (b) after administration of gadoxetic acid. The images demonstrate an hepatic haemangioma in hepatic segment VIII (arrows), which shows high signal intensity on both (a) and (b). Both readers correctly interpreted these lesions as non-solid lesions on both non-enhanced and gadoxetic acid-enhanced images. (c, d) Fat-saturated, single-shot, echo-planar, diffusion weighted axial images (TR/TE, 4000 ms/80 ms; *b*-factor, 50 s mm$^{-2}$) obtained (c) before and (d) after administration of gadoxetic acid show the same high-signal lesion (arrows).

remained in the hepatic parenchyma in a high concentration [8, 23, 24]. Lesion-to-liver CNR was significantly improved on gadoxetic acid-enhanced DW images compared with non-enhanced DW images. This might have been caused by the lack of hepatobiliary uptake of gadoxetic acid in focal hepatic lesions without functioning hepatocytes, thus resulting in more pronounced signal reduction of the hepatic parenchyma than of focal hepatic lesions on gadoxetic acid-enhanced DW images [4, 5]. However, conflicting results were noted for $T_2$ weighted imaging, which showed similar lesion-to-liver CNR for non-enhanced and gadoxetic acid-enhanced $T_2$ weighted images. This discrepancy could have resulted from different delay times for $T_2$ weighted and DW imaging after administration of gadoxetic acid (*i.e.* an approximate 4 min delay for $T_2$ weighted imaging and an approximate 11 min delay for DW imaging). Because the hepatic concentration of gadoxetic acid gradually increases until reaching peak hepatic enhancement 20 min after contrast injection [5, 8], the hepatic concentration of gadoxetic acid might have been higher at the time of DW imaging than on $T_2$ weighted imaging. This factor probably led to a greater reduction of hepatic parenchymal SI and in turn a greater improvement of lesion-to-liver

**Table 4.** Results of quantitative analysis of liver SI, background noise, liver SNR and lesion-to-liver CNR of focal hepatic lesions

| | $T_2$ weighted imaging | | | Diffusion weighted imaging | | |
|---|---|---|---|---|---|---|
| | Non-enhanced | Gadoxetic acid-enhanced | *p*-values | Non-enhanced | Gadoxetic acid-enhanced | *p*-values |
| Liver SI[a] | 81.4±27.9 | 72.2±22.7 | <0.001 | 63.2±22.2 | 55.6±18.7 | <0.001 |
| Background noise[a] | 3.8±1.2 | 4.0±1.2 | 0.04 | 1.4±0.6 | 1.4±0.6 | 0.82 |
| Liver SNR[a] | 24.4±13.5 | 20.2±10.1 | <0.001 | 58.8±26.5 | 46.4±22.1 | <0.001 |
| CNR of all lesions (*n*=87) | 35.9±29.2 | 35.1±30.0 | 0.65 | 87.8±85.0 | 92.6±98.3 | 0.02 |
| CNR of solid lesions (*n*=60) | 24.3±21.8 | 25.1±24.1 | 0.62 | 66.0±62.9 | 78.1±91.6 | 0.04 |
| CNR of non-solid lesions (*n*=27) | 61.4±27.5 | 57.2±30.2 | 0.32 | 137.0±106.8 | 145.0±98.6 | 0.37 |

CNR, contrast-to-noise ratio; SI, signal intensity; SNR, signal-to-noise ratio.
Data are means ± standard deviation.
[a]The total sample size was 63 patients.

CNR on gadoxetic acid-enhanced DW images compared with $T_2$ weighted images. Moreover, as DW imaging using an echo planar sequence is known to be more sensitive to $T_2$* decay than $T_2$ weighted imaging using a turbo spin-echo sequence [25], the $T_2$* shortening effect of gadolinium in the hepatic parenchyma might have induced an additional loss of liver SI and in turn led to a greater increase in lesion-to-liver contrast on DW images than on $T_2$ weighted images.

Another noteworthy finding of our study was that the ADC values of focal hepatic lesions measured on gadoxetic acid-enhanced DW images did not differ significantly from those measured on non-enhanced images. Considering the results of recent studies showing the value of quantitative ADC measurement for characterising hepatic lesions and for monitoring the therapeutic response of malignant hepatic tumours [26, 27], our results could have clinical implications. Our observations suggest that the ADC values of focal hepatic lesions measured on gadoxetic acid-enhanced DW images might be used instead of those measured on standard, non-enhanced DW images.

Overall, our data suggests that gadoxetic acid-enhanced $T_2$ weighted and DW imaging might be able to replace standard, non-enhanced $T_2$ weighted and DW imaging without any adverse effect on the diagnostic accuracy or image quality. Therefore, it is feasible to acquire $T_2$ weighted and DW images during the time gap between dynamic contrast-enhanced $T_1$ weighted imaging and hepatobiliary phase imaging. Using this modified MRI protocol, the examination time can be shortened by as much as the time required for $T_2$ weighted and DW imaging (*i.e.* approximately 10 min in our study).

Our study does have limitations. Firstly, only a small number of hepatic lesions were pathologically confirmed. Pathological proof of all lesions would have provided more reliable reference-standard data; however, this might not have been crucial for our study, as its main purpose was not to evaluate the accuracy of an imaging technique in lesion characterisation. Instead, we aimed to evaluate the effect of contrast enhancement on the image quality and the readers' interpretation of MRI compared with standard, non-enhanced images. Secondly, we did not evaluate the effect of gadoxetic acid on the ADC values of the normal hepatic parenchyma. Given a significant reduction in liver SI on DW images after administration of gadoxetic acid in our study, its effect on the ADC values of the hepatic parenchyma should be determined by further research.

In conclusion, acquisition of $T_2$ weighted and DW images after administration of gadoxetic acid has no significant effect on detecting and characterising focal hepatic lesions, although it does improve the lesion-to-liver CNR on DW images. Therefore, for time-efficient, gadoxetic acid-enhanced liver MRI examinations, it is preferable to obtain $T_2$ weighted and DW images during the interval between the contrast-enhanced dynamic imaging and the hepatobiliary phase imaging.

## Acknowledgments

This study was supported by a grant (2008-444) from the Asan Institute for Life Sciences, Seoul, Republic of Korea.

## References

1. Halavaara J, Breuer J, Ayuso C, Balzer T, Bellin MF, Blomqvist L, et al. Liver tumor characterization: comparison between liver-specific gadoxetic acid disodium-enhanced MRI and biphasic CT – a multicenter trial. J Comput Assist Tomogr 2006;30:345–54.
2. Hammerstingl R, Huppertz A, Breuer J, Balzer T, Blakeborough A, Carter R, et al. Diagnostic efficacy of gadoxetic acid (Primovist)-enhanced MRI and spiral CT for a therapeutic strategy: comparison with intraoperative and histopathologic findings in focal liver lesions. Eur Radiol 2008;18:457–67.
3. Huppertz A, Balzer T, Blakeborough A, Breuer J, Giovagnoni A, Heinz-Peer G, et al. Improved detection of focal liver lesions at MR imaging: multicenter comparison of gadoxetic acid-enhanced MR images with intraoperative findings. Radiology 2004;230:266–75.
4. Huppertz A, Haraida S, Kraus A, Zech CJ, Scheidler J, Breuer J, et al. Enhancement of focal liver lesions at gadoxetic acid-enhanced MR imaging: correlation with histopathologic findings and spiral CT – initial observations. Radiology 2005;234:468–78.
5. Vogl TJ, Kummel S, Hammerstingl R, Schellenbeck M, Schumacher G, Balzer T, et al. Liver tumors: comparison of MR imaging with Gd-EOB-DTPA and Gd-DTPA. Radiology 1996;200:59–67.
6. Zech CJ, Grazioli L, Breuer J, Reiser MF, Schoenberg SO. Diagnostic performance and description of morphological features of focal nodular hyperplasia in Gd-EOB-DTPA-enhanced liver magnetic resonance imaging: results of a multicenter trial. Invest Radiol 2008;43:504–11.
7. Zech CJ, Herrmann KA, Reiser MF, Schoenberg SO. MR imaging in patients with suspected liver metastases: value of liver-specific contrast agent Gd-EOB-DTPA. Magn Reson Med Sci 2007;6:43–52.
8. Hamm B, Staks T, Muhler A, Bollow M, Taupitz M, Frenzel T, et al. Phase I clinical evaluation of Gd-EOB-DTPA as a hepatobiliary MR contrast agent: safety, pharmacokinetics, and MR imaging. Radiology 1995;195:785–92.
9. Reimer P, Rummeny EJ, Daldrup HE, Hesse T, Balzer T, Tombach B, et al. Enhancement characteristics of liver metastases, hepatocellular carcinomas, and hemangiomas with Gd-EOB-DTPA: preliminary results with dynamic MR imaging. Eur Radiol 1997;7:275–80.
10. Kanematsu M, Hoshi H, Itoh K, Murakami T, Hori M, Kondo H, et al. Focal hepatic lesion detection: comparison of four fat-suppressed T2-weighted MR imaging pulse sequences. Radiology 1999;211:363–71.
11. Lee SS, Byun JH, Hong HS, Park SH, Won HJ, Shin YM, et al. Image quality and focal lesion detection on T2-weighted MR imaging of the liver: comparison of two high-resolution free-breathing imaging techniques with two breath-hold imaging techniques. J Magn Reson Imaging 2007;26:323–30.
12. Parikh T, Drew SJ, Lee VS, Wong S, Hecht EM, Babb JS, et al. Focal liver lesion detection and characterization with diffusion-weighted MR imaging: comparison with standard breath-hold T2-weighted imaging. Radiology 2008; 246:812–22.
13. Malone D, Zech CJ, Ayuso C, Bartolozzi C, Jonas E, Tanimoto A. Magnetic resonance imaging of the liver: consensus statement from the 1st International Primovist User Meeting. Eur Radiol 2008;18:D1–16.
14. Kim YK, Kwak HS, Kim CS, Han YM. Detection and characterization of focal hepatic tumors: a comparison of $T_2$-weighted MR images before and after the administration of gadoxetic acid. J Magn Reson Imaging 2009;30: 437–43.
15. Chang SD, Thoeni RF. Effect of T1 shortening on T2-weighted MRI sequences: comparison of hepatic mass conspicuity on

images acquired before and after gadolinium enhancement. AJR Am J Roentgenol 2008;190:1318–23.
16. Jeong YY, Mitchell DG, Holland GA. Liver lesion conspicuity: T2-weighted breath-hold fast spin-echo MR imaging before and after gadolinium enhancement – initial experience. Radiology 2001;219:455–60.
17. Hirokawa Y, Isoda H, Maetani YS, Arizono S, Shimada K, Okada T, et al. Hepatic lesions: improved image quality and detection with the periodically rotated overlapping parallel lines with enhanced reconstruction technique – evaluation of SPIO-enhanced T2-weighted MR images. Radiology 2009;251:388–97.
18. Lee SS, Byun JH, Park BJ, Park SH, Kim N, Park B, et al. Quantitative analysis of diffusion-weighted magnetic resonance imaging of the pancreas: usefulness in characterizing solid pancreatic masses. J Magn Reson Imaging 2008; 28:928–36.
19. Chakraborty D, Yoon HJ, Mello-Thoms C. Spatial localization accuracy of radiologists in free-response studies: inferring perceptual FROC curves from mark-rating data. Acad Radiol 2007;14:4–18.
20. Altman DG. Some common problems in medical research. In: Altman DG, ed. Practical statistics for medical research. London, UK: Chapman & Hall, 1991: 403–8.
21. Martin J, Puig J, Darnell A, Donoso L. Magnetic resonance of focal liver lesions in hepatic cirrhosis and chronic hepatitis. Semin Ultrasound CT MR 2002;23:62–78.
22. Kim YK, Kim CS, Moon WS, Cho BH, Lee SY, Lee JM. MRI findings of focal eosinophilic liver diseases. AJR Am J Roentgenol 2005;184:1541–8.
23. Lin SP, Brown JJ. MR contrast agents: physical and pharmacologic basics. J Magn Reson Imaging 2007;25:884–99.
24. Reimer P, Schneider G, Schima W. Hepatobiliary contrast agents for contrast-enhanced MRI of the liver: properties, clinical development and applications. Eur Radiol 2004;14:559–78.
25. Le Bihan D, Poupon C, Amadon A, Lethimonnier F. Artifacts and pitfalls in diffusion MRI. J Magn Reson Imaging 2006;24:478–88.
26. Bruegel M, Holzapfel K, Gaa J, Woertler K, Waldt S, Kiefer B, et al. Characterization of focal liver lesions by ADC measurements using a respiratory triggered diffusion-weighted single-shot echo-planar MR imaging technique. Eur Radiol 2008;18:477–85.
27. Chen CY, Li CW, Kuo YT, Jaw TS, Wu DK, Jao JC, et al. Early response of hepatocellular carcinoma to transcatheter arterial chemoembolization: choline levels and MR diffusion constants – initial experience. Radiology 2006;239: 448–56.